

Design of Linear Control System for Wind Turbine Blade Fatigue Testing

Anders Toft¹, Bjarke Roe-Poulsen², Rasmus Christiansen³ and Torben Knudsen⁴

Dept. of Electronic Systems, Sec. of Automation and Control, Aalborg University
Fredrik Bajers Vej 7C, 9220 Aalborg East, DK

E-mail: {¹atoft11, ²broepo11, ³rchr12}@student.aau.dk and ⁴tk@es.aau.dk

Abstract.

This paper proposes a linear method for wind turbine blade fatigue testing at Siemens Wind Power. The setup consists of a blade, an actuator (motor and load mass) that acts on the blade with a sinusoidal moment, and a distribution of strain gauges to measure the blade flexure. Based on the frequency of the sinusoidal input, the blade will start oscillating with a given gain, hence the objective of the fatigue test is to make the blade oscillate with a controlled amplitude. The system currently in use is based on frequency control, which involves some non-linearities that make the system difficult to control. To make a linear controller, a different approach has been chosen, namely making a controller which is not regulating on the input frequency, but on the input amplitude.

A non-linear mechanical model for the blade and the motor has been constructed. This model has been simplified based on the desired output, namely the amplitude of the blade. Furthermore, the model has been linearised to make it suitable for linear analysis and control design methods.

The controller is designed based on a simplified and linearised model, and its gain parameter determined using pole placement. The model variants have been simulated in the MATLAB toolbox Simulink, which shows that the controller design based on the simple model performs adequately with the non-linear model. Moreover, the developed controller solves the robustness issue found in the existent solution and also reduces the needed energy for actuation as it always operates at the blade eigenfrequency.

1. Introduction

In order to guarantee continuous operation for its required lifespan, wind turbine blades from Siemens Wind Power are subject to thorough testing. One of such tests is a fatigue test, which is used as a random check of the structural integrity of the blade at an extended period of time. So far, Siemens have been using a method for fatigue testing using a motor with a mass extended by a connection rod. This is mounted directly on the blade, and through rotation causes the blade to oscillate. In the mechanical nature of the blade, as interpreted in figure 1, a periodic excitation will, after some time, cause the blade to oscillate at the same frequency, for which the amplitude of deformation depends on the system gain and the input amplitude. The maximum amplitude of deformation is at the mechanical eigenfrequency (first mode) of the blade, as illustrated in figure 2, and is the point where the least energy is needed to achieve a given amplitude.[1] At the time of writing, Siemens use a feedback control loop, taking an



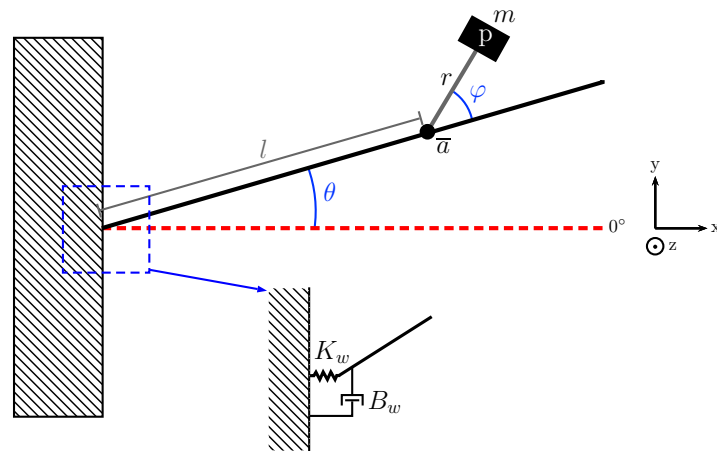


Figure 1. General overview of the physical structure.

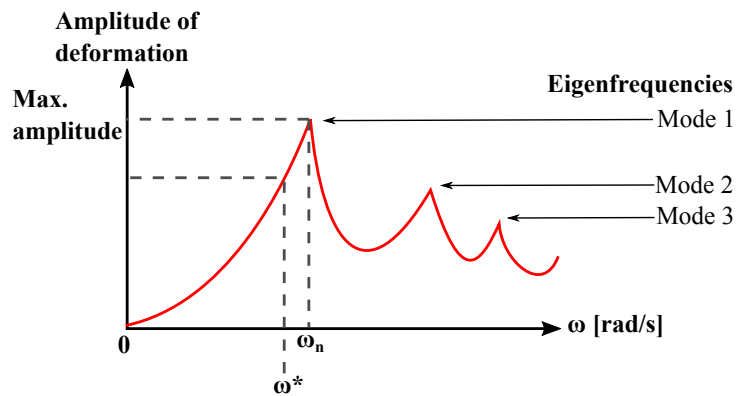


Figure 2. Current system principle of operation with desired frequency ω^* and natural eigenfrequency ω_n .

oscillation amplitude reference value and comparing it to the current amplitude. The error is then used to alter the frequency at which the motor rotates. The U.S. National Renewable Energy Laboratory uses a similar method, where hydraulic pistons are used instead of a motor to provide a sinusoidal input moment [2]. An apparent issue with both these methods is that, should the eigenfrequency be exceeded, the controller will see this as a positive error and increase the motor frequency further, which decreases the gain and causes the test to fail as it can not recover.

This paper examines a different approach where the actuator is assumed to have a variable connection rod length, letting this control the excitation force when the motor is already running at the eigenfrequency. If the exciter mass is moving at a circle with constant speed the centrifugal force amplitude is $F = m \cdot \omega \cdot r$ i.e. linear in r . The key idea in this paper is that using r as the control input the system will be sufficiently close to linear to apply linear control system analysis and design. Thus, the results of this paper will be a control system based on the actuation shown in figures 3 and 4, and a controller designed to suit the requirements.

Section 2 describes the methods that are used to analyse and model the system, section 3 describes the controller design procedure and section 4 describes the method used to estimate the amplitude of the non-linear model. In section 5, simulations with the designed control system are presented. Finally, in section 6, different aspects of the content of the paper are discussed

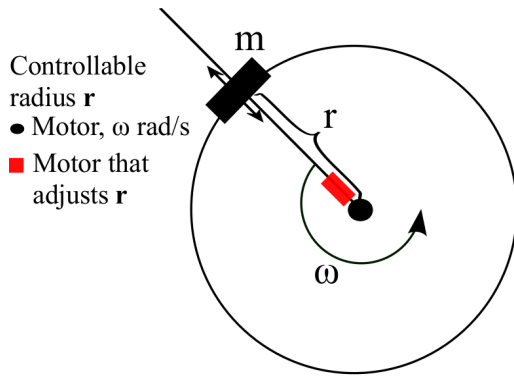


Figure 3. Alternative system principle of operation with variable rod length r .

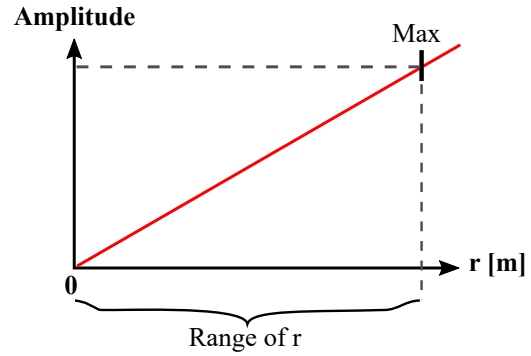


Figure 4. Alternative system characteristics.

for alternative approaches etc.

Table 1 lists the basic variables and constants used in this paper, with a small description and units. In this, and throughout this paper, vectors will be denoted with bars (e.g. \bar{z}), ma-

Table 1. Common variables and constants in this paper

Variables		
$\theta(t)$	Angle between blade tip and base	$[rad]$
$\dot{\theta}(t)$	Angular velocity	$[rad/s]$
$\ddot{\theta}(t)$	Angular acceleration	$[rad/s^2]$
$\varphi(t)$	Actuator angle to blade	$[rad]$
ω	Actuator angular velocity	$[rad/s]$
$r(t)$	Actuator connection rod length	$[m]$
$\bar{p}(t)$	Actuator load mass point	$[m]$
\bar{a}	Actuator mounting point	$[m]$
\bar{F}_τ	Actuator force	$[N]$
Constants		
l	Distance from blade base to actuator mount, equal to $ \bar{a} $	$[m]$
m	Actuator load mass	$[kg]$
τ_m	Actuator input moment	$[Nm]$
J_w	Blade mass inertia	$[Nm \cdot s^2]$
D_w	Non-linear drag coefficient	$[Nm \cdot s^2]$
$D_{w,lin}$	Linearised drag coefficient	$[Nm \cdot s]$
K_i	Controller integrator coefficient	$[-]$

trices with capital letters and double-bars ($\bar{\bar{Z}}$), time derivatives with dots (\dot{z}) and double time derivatives with double-dots (\ddot{z}).

2. Modelling

To cope with the challenge of controlling the amplitude of the blade in a linear manner, the procedure is:

- Model the plant and identify the possible non-linearities.
- Simplify and linearise the model.
- Design a control system for the simplified and linearised system.
- Implement the controller in the non-simplified and non-linearised system.

This procedure will work as a guideline throughout this paper.

Figure 1 shows the interpretation of the system mechanics, i.e. a stiff beam with the coefficients listed in table 1.

This interpretation results in equation (1) which is the mechanical moment equilibrium of the blade.

$$J_w \cdot \ddot{\theta}(t) = \tau_m - D_w \cdot \dot{\theta}^2(t) \cdot \text{sgn}(\dot{\theta}(t)) - K_w \cdot \theta(t), \quad (1)$$

It has been derived under the assumption that the damping coefficient B_w is negligible. Instead, aerodynamic drag is included with the term $D_w \cdot \dot{\theta}^2$, due to the physical size of the blade. The coefficient D_w depends on several factors, such as air density, the area facing the direction of movement and the shape of the body.

The term $D_w \cdot \dot{\theta}^2(t) \cdot \text{sgn}(\dot{\theta}(t))$ ¹ in equation (1) is found by analysis of the aerodynamics of the blade in the relevant direction, although this will not be covered in this paper. Linearising the term as a straight line between two bounds, found through simulations to be ± 4 rad/s, and inserting this into equation (1) yields:

$$J_w \cdot \ddot{\theta}(t) = \tau_m - D_{w,lin} \cdot \dot{\theta}(t) - K_w \cdot \theta(t), \quad (2)$$

where $D_{w,lin}$ is the approximation coefficient. This linearisation is illustrated in figure 5. [1]

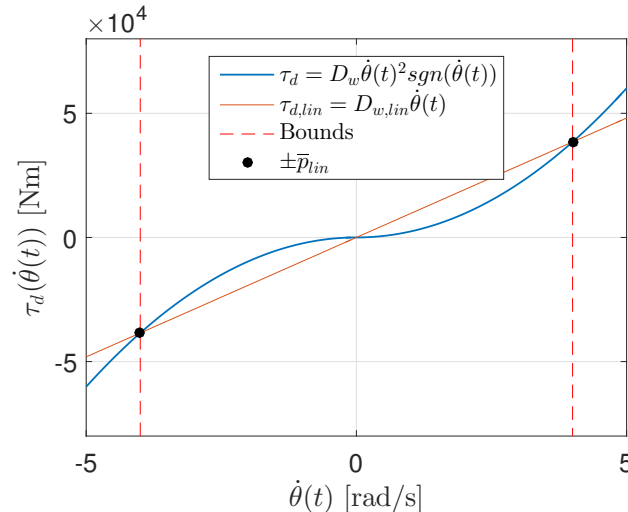


Figure 5. Linearisation of drag moment τ_d with linearisation bounds ± 4 rad/s

With the linearised model of the blade in equation (2), the input τ_m is derived. Considering the actuator at constant ω , the fictitious centrifugal force is acting upon the point \bar{a} , which creates a moment on the blade. However, since the actuator moves with the blade, additional terms are expected, such as the fictitious Euler force. In order to properly analyse

¹ The *signum* function: $\text{sgn}(x) = \frac{x}{|x|}$, $x \neq 0$ and $\text{sgn}(0) = 0$.

the applied moment, the acceleration $\ddot{\bar{p}}(t)$ is described in terms of $\theta(t)$ and $\varphi(t)$, with $\bar{p}(t)$ given by equation (3):

$$\bar{p}(t) = l \cdot \begin{bmatrix} \cos(\theta(t)) \\ \sin(\theta(t)) \end{bmatrix} + r(t) \cdot \begin{bmatrix} \cos(\varphi(t) + \theta(t)) \\ \sin(\varphi(t) + \theta(t)) \end{bmatrix} \quad (3)$$

The moment induced at the anchor point of the blade is defined as the cross product of the excitation force \bar{F}_τ and the blade up to point \bar{a} :

$$\begin{aligned} \tau_m &= \bar{a} \times \bar{F}_\tau = \bar{a} \times (-m \cdot \ddot{\bar{p}}(t)) \\ &= l \cdot m \cdot r(t) \cdot \sin(\omega \cdot t) \cdot (\omega + \dot{\theta}(t))^2 \\ &\quad - (l^2 \cdot m + l \cdot m \cdot r(t) \cdot \cos(\omega \cdot t)) \cdot \ddot{\theta}(t), \end{aligned} \quad (4)$$

Assuming that contributions from the angular velocity of the blade, $\dot{\theta}(t)$, and the variation of inertia due to the movement of the actuator mass, $l \cdot m \cdot r(t) \cdot \cos(\omega \cdot t) \cdot \ddot{\theta}(t)$, are negligible, equation (4) reduces to:

$$\tau_m = G_i \cdot r(t) \cdot \sin(\omega t) - l^2 \cdot m \cdot \ddot{\theta}(t), \quad (5)$$

where $G_i = l \cdot m \cdot \omega^2$. Here, it is seen that the last term of τ_m is a contribution to the inertia, hence it can be added to J_w and omitted from τ_m . This observation results in the following expression for the combined inertia: $J_c = J_w + l^2 \cdot m$, and the reduced moment, $\tau_r = G_i \cdot r(t) \cdot \sin(\omega t)$. By inserting J_c and τ_r in equation (1), taking the Laplace transform and arranging it according to the second order transfer function standard form, equation (6) is obtained:

$$G_w(s) = \frac{\theta(s)}{\tau_r(s)} = G_k \cdot \frac{\omega_n^2}{s^2 + 2 \cdot \omega_n \cdot \zeta \cdot s + \omega_n^2}, \quad (6)$$

where

$$\begin{aligned} \omega_n &= \sqrt{\frac{K_w}{J_c}} && \text{is the mechanical eigenfrequency,} \\ \zeta &= \frac{D_{w,lin}}{2 \cdot \sqrt{J_c \cdot K_w}} && \text{is the damping ratio and} \\ G_k &= \frac{1}{K_w} && \text{is the system gain} \end{aligned}$$

In order to design a control system for the amplitude, the model must be simplified to output this.

An underdamped dynamic system subject to a sine wave input will also output a sine wave, with an amplitude gain and a phase shift dependent on the system characteristics. The imaginary parts of the complex system poles describe these oscillations. The real parts, on the other hand, describe the dynamics of the amplitude, as seen on figure 6.

It is thus possible to describe the oscillation amplitude by a first order system with a pole equal to the aforementioned real parts of the complex poles and the system gain at the given frequency:

$$\frac{A(s)}{\tau_{ra}(s)} = |G_w(j\omega_n)| \cdot G_{1.order}(s), \quad (7)$$

where

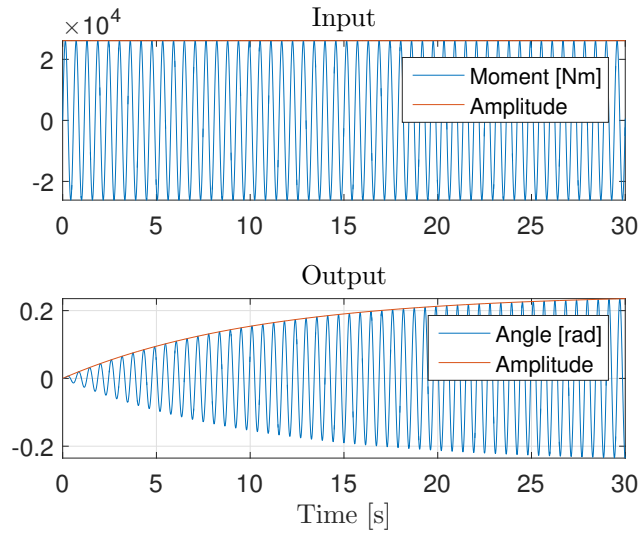


Figure 6. Output response for given sine input.

$$\begin{array}{ll}
 A(s) : \text{Amplitude of the blade oscillations} & [rad] \\
 \tau_{ra}(s) : \text{Amplitude of the sine input } \tau_r & [Nm] \\
 |G_w(j\omega_n)| : \text{Gain of } G_w \text{ at the eigenfrequency} & [(Nm)^{-1}] \\
 G_{1.order} : \text{First order system dynamics} & [-]
 \end{array}$$

The real parts of the poles in equation (6) are $-\zeta \cdot \omega_n$. As the amplitude input can be expressed as $\tau_{ra}(s) = G_i \cdot r(s)$, by letting $r(s)$ be the system input, equation (7) becomes:

$$\begin{aligned}
 G_{amp} &= \frac{A(s)}{r(s)} = G_i \cdot |G_w(j\omega_n)| \cdot G_{1.order} & (8) \\
 &= l \cdot m \cdot \omega_n^2 \cdot \frac{1}{K_w} \cdot \frac{1}{2 \cdot \zeta} \cdot \frac{\zeta \omega_n}{s + \zeta \omega_n} \\
 &= \frac{l \cdot m \cdot \omega_n^3}{2 \cdot K_w} \cdot \frac{1}{s + \zeta \cdot \omega_n} = \frac{b}{s + c}
 \end{aligned}$$

This will be the basis for the controller design.

3. Controller Design

From equation (8), a controller is designed through pole-placement with respect to the requirements. It is seen from equation (8) that the system is of type 0, thus an integrator is needed to properly eliminate steady-state errors. From the approximation of the settling time defined within $\pm 2\%$ of the steady-state value, $T_s \approx \frac{4}{c}$, the desired pole location c^* is given by [1]:

$$c^* = -\frac{4}{T_s} \quad (9)$$

This can be achieved with the controller given by

$$C(s) = \frac{K_i}{s}, \quad (10)$$

where K_i is the integration gain. The closed loop transfer function with this controller becomes

$$G_{CL}(s) = \frac{K_i \cdot b}{s^2 + c \cdot s + K_i \cdot b} = \frac{K_i \cdot b}{Q(s)}, \quad (11)$$

where $Q(s)$ is the characteristic equation of the closed loop system. Solving this for K_i and inserting the desired pole location c^* yields the required gain to place the closed loop poles such that the response satisfies the requirement for T_s :

$$K_i = \frac{-(c^*)^2 - c \cdot c^*}{b}, \quad (12)$$

where b and c are defined in equation (8). [1] The resulting control system is shown in figure 7.

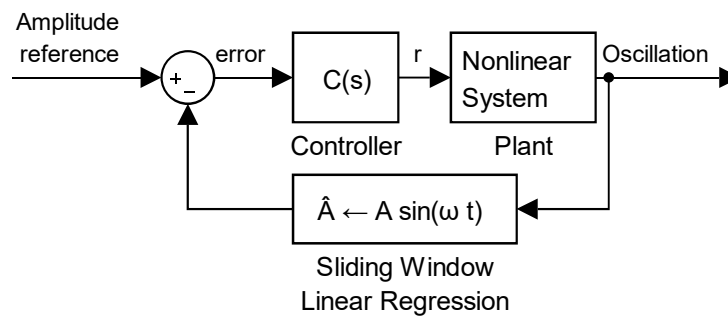


Figure 7. Control system architecture

4. Amplitude Estimation

In order to use the controller with the non-linear model, the amplitude of the oscillating output is needed. In this paper, the output $\theta(t)$ is approximated as a sine wave by linear regression, such that:

$$\theta(t) \approx A_1 \sin(\omega t) + A_2 \cos(\omega t) + D, \quad (13)$$

where A is the amplitude, ω is the angular velocity, t is time and D is the error. As $\theta(t)$ is the model output, and ω is predefined, taking N samples yields the set of equations:

$$\begin{bmatrix} \theta_1 \\ \theta_2 \\ \vdots \\ \theta_N \end{bmatrix} \approx \begin{bmatrix} \sin(\omega_1 \cdot t_1) & \cos(\omega_1 \cdot t_1) & 1 \\ \sin(\omega_2 \cdot t_2) & \cos(\omega_2 \cdot t_2) & 1 \\ \vdots & \vdots & \vdots \\ \sin(\omega_N \cdot t_N) & \cos(\omega \cdot t_N) & 1 \end{bmatrix} \begin{bmatrix} A_1 \\ A_2 \\ D \end{bmatrix} = \overline{\overline{M}} \cdot \bar{x} \quad (14)$$

A solution to this system of equations is, by least squares [3]:

$$\bar{x} = \left(\overline{\overline{M}}^T \cdot \overline{\overline{M}} \right)^{-1} \cdot \overline{\overline{M}}^T \cdot \bar{\theta}, \quad (15)$$

where $\bar{\theta}$ is the vector of N samples of $\theta(t)$.
 The estimate of the amplitude, \hat{A} , is then:

$$\hat{A} = \sqrt{x_1^2 + x_2^2} = \sqrt{A_1^2 + A_2^2} \quad (16)$$

By limiting the number of samples and using the First In First Out principle, a sliding window of N samples is used, allowing the estimation to follow variations in the amplitude.

5. Results

With the designed controller, $C(s) = \frac{K_i}{s}$, the closed-loop system step response is shown in figure 8 (yellow) along with some simpler controller alternatives, i.e. unit gain (blue) and a unit gain, free integrator (red). c_{ss} is the steady-state value, for which the settling time is defined as when the transient response reaches $\pm 2\%$ of this value (dashed lines in figure 8). It is seen that the

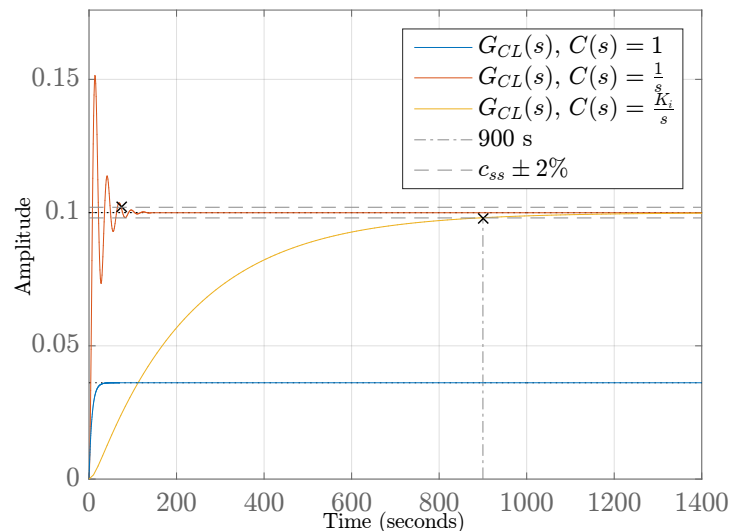


Figure 8. System step response with different controllers and G_{amp} . The dash-dotted line indicates the required settling time.

controller performs as intended with the simplified and linearised system, given the requirements in table 3. For the non-linear, non-simplified system, a simulation with the parameters given in table 2 yields a response as seen in figure 9.

Figure 9 shows the amplitude estimated by regression, \hat{A} , which matches the peaks of θ adequately. Regarding the controller performance, figure 10 shows a comparison of a step input of 0.1 rad for both the simplified system and the non-linear model. The deviation between the two model variants is small for the same controller and reference. As such, it is possible to conclude that the assumptions made in order to reduce equation (4) to equation (5) have had only a minor effect on the usefulness of the controller.

6. Discussion

When controlling the amplitude of the blade, the distance from the motor to the actuator load mass is limited by the length of the connection rod. This gives the risk of saturation, where the actuator output cannot be larger. Therefore, larger driving moments can only be achieved by moving the actuator mounting point (\bar{a}), or alternatively increasing the maximum length of

Table 2. Specific parameters for simulation in figures 9 and 10

Name	Size	Unit
$r(t)$	$\in [0, 1]$	$[m]$
J_w	45119	$[kg \cdot m^2]$
K_w	$5.946 \cdot 10^6$	$[N \cdot m]$
D_w	$2.405 \cdot 10^3$	$[kg \cdot m^2]$
$D_{w,lin}$	$9.620 \cdot 10^3$	$[kg \cdot m^2 \cdot s^{-1}]$
l	10	$[m]$
m	50	$[kg]$
p_{lin}	$\pm 438.48 \cdot 10^3$	$[rad \cdot s^{-1}, Nm]$
K_i	0.0057	$[-]$
c	0.09597	$[-]$
b	0.05433	$[-]$

Table 3. System control requirements

Name	Size	Unit
T_s	$\in [600, 1200]$	$[s]$
e_{ss}	0	$[\%]$
M_p	0	$[\%]$

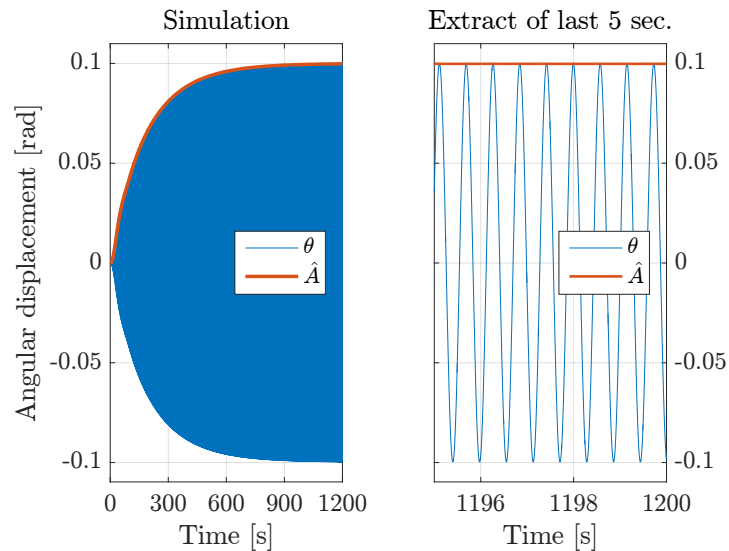


Figure 9. Left: Simulation of non-linear model with controller and setpoint 0.1, as well as estimated amplitude \hat{A} . Right: Close up look at the final five seconds.

the arm or manually increasing the actuator mass, but this takes up space and at some point exceeds what is physically feasible. An alternative option is to control the mass instead (or along with) of the distance to it, e.g. by using a pump supplying water to a ballast tank.

Regarding the estimation of the amplitude, the approach taken in this project, namely regression by least squares, is only one example of how this can be achieved. Least squares can be improved by solving the set of equation by total least squares or recursive least squares regression instead, but since the estimation is not the primary goal of the project neither of these has been implemented.[4] An alternative solution would be some methods of direct measurement

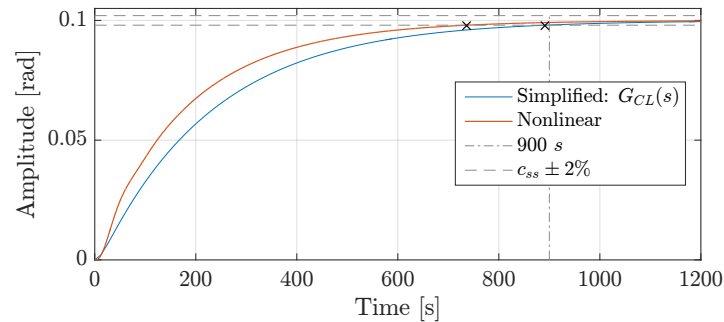


Figure 10. Comparison of the simplified system and the non-linear model simulation, both with identical control.

of the amplitude, as this would give an exact value instead of an estimation, though this is not possible unless a physical system is available.

The results further show a working concept of a controller of the form $C(s) = \frac{K_i}{s}$, i.e. an I-controller. It was found that this topology was enough to fulfil the requirements, and thus e.g. a PI-controller was not needed. For another system, such as a larger blade, the controller design and topology choice should be reconsidered, as the simple controller presented in this paper may not be sufficient.

The simulations presented in this paper show that the control system designed for the fatigue test is working as intended. Additionally, the robustness problem found in the existing controller is solved by the developed one and actuation energy savings are possible from operating constantly at the first blade frequency. In order to verify these conclusions, a test setup would be necessary to support them with experimental data.

Acknowledgements

Thanks to Siemens Wind Power for the collaboration and especially thanks to Søren Christiansen (*Siemens Wind Power*) for providing the needed information about blade construction and the current testing facility.

References

- [1] Phillips C L and Parr J M 2011 *Feedback Control Systems* 5th ed (Pearson Education)
- [2] White D 2004 *New Method for Dual-Axis Fatigue Testing of Large Wind Turbine Blades Using Resonance Excitation and Spectral Loading* Tech. rep. National Renewable Energy Laboratory (NREL), U.S. Department of Energy URL <http://www.nrel.gov/docs/fy04osti/35268.pdf>
- [3] Selesnick I 2013 *Least Squares with Examples in Signal Processing* Lecture note
- [4] Xin W and Yuanyuan X 2010 *3rd International Conference on Advanced Computer Theory and Engineering (ICACTE)*